# Lawrence Berkeley National Laboratory
## Materials Sciences

**Title**
Reaction chemistry in rechargeable Li–O 2 batteries

**Permalink**
https://escholarship.org/uc/item/3fc0j95b

**Journal**
Chemical Society Reviews, 46(10)

**ISSN**
0306-0012

**Authors**
Lim, Hee-Dae
Lee, Byungju
Bae, Youngjoon
et al.

**Publication Date**
2017-05-22

**DOI**
10.1039/c6cs00929h

Peer reviewed

# Chem Soc Rev

Check for updates

# Reaction chemistry in rechargeable Li–O₂ batteries

Hee-Dae Lim,†[a] Byungju Lee,†[a] Youngjoon Bae,[a] Hyeokjun Park,[a] Youngmin Ko,[a] Haegyeom Kim,‡[a] Jinsoo Kim§[a] and Kisuk Kang ⓘ *[ab]

The seemingly simple reaction of Li–O₂ batteries involving lithium and oxygen makes this chemistry attractive for high-energy-density storage systems; however, achieving this reaction in practical rechargeable Li–O₂ batteries has proven difficult. The reaction paths leading to the final Li₂O₂ discharge products can be greatly affected by the operating conditions or environment, which often results in major side reactions. Recent research findings have begun to reveal how the reaction paths may be affected by the surrounding conditions and to uncover the factors contributing to the difficulty in achieving the reactions of lithium and oxygen. This progress report describes the current state of understanding of the electrode reaction mechanisms in Li–O₂ batteries; the factors that affect reaction pathways; and the effect of cell components such as solvents, salts, additives, and catalysts on the discharge product and its decomposition during charging. This comprehensive review of the recent progress in understanding the reaction chemistry of the Li–O₂ system will serve as guidelines for future research and aid in the development of reliable high-energy-density rechargeable Li–O₂ batteries.

[a] *Department of Materials Science and Engineering, Research Institute of Advanced Materials (RIAM), Seoul National University, 1 Gwanak-ro, Gwanak-gu, Seoul 151-742, Republic of Korea. E-mail: matlgen1@snu.ac.kr*
[b] *Center for Nanoparticle Research, Institute for Basic Science (IBS), Seoul National University, 1 Gwanak-ro, Gwanak-gu, Seoul 151-742, Republic of Korea*
† These authors contributed equally to this work.
‡ Present address: Lawrence Berkeley National Laboratory, 1 Cyclotron Road, Berkeley, California, 94720, USA.
§ Present address: Division of Automotive Research and Development, Hyundai Motor Company, 37 Cheoldobangmulgwan-ro, Uiwang, Gyeonggi-do, 437-815, Republic of Korea.

The demand for high-energy-density energy storage systems has been rapidly growing with advances in technologies such as electric vehicles and mobile electronic devices. Li-ion batteries (LIBs) have served as a major power option but are reaching their maximum capacities, which are limited by the intercalation chemistry. Tremendous research efforts have thus been devoted to the search for a new energy storage system that can outperform state-of-the-art LIBs. As one of such candidates, Li–O₂ batteries have attracted considerable attention because of their high theoretical energy densities ($\sim$3500 W h kg$^{-1}$),

*Hee-Dae Lim received a BSc in the department of materials science and engineering from Hanyang University (2010) and an MSc in the graduate school of EEWS from the Korea Advanced Institute of Science and Technology (KAIST) in 2011. He obtained his PhD from Seoul National University in 2016 under the supervision of prof. Kisuk Kang and Jang Wook Choi. Currently, he is a post-doctoral research fellow at University of California, San Diego in Ping Liu's research group. His research interests are focused on next generation metal–gas batteries and all solid state batteries.*

**Hee-Dae Lim**

*Byungju Lee is a PhD candidate under the supervision of prof. Kisuk Kang at Seoul National University (SNU). He received a BSc. and MSc in the department of materials science and engineering at SNU. He has been interested in elucidating reaction mechanism of metal–oxygen batteries, using density functional theory (DFT) calculations. His research interest also covers theoretical analysis of organic-based electrode materials and advanced Li-ion batteries.*

**Byungju Lee**

which are among the highest for known battery chemistries.[1–3] This high energy density can be attributed to the simple reaction between oxygen and lithium ions, $2Li^+ + O_2 + 2e^- \rightarrow Li_2O_2$, which does not require any heavy transition metals or intercalation frameworks.[4,5] Furthermore, the use of the environmentally friendly and unlimited source of oxygen makes this chemistry more attractive as a next-generation energy storage system. However, despite its great promise, the current state of Li–O$_2$ batteries has been seriously plagued by several critical issues that must be addressed. The electrolyte instability, degradation of the air electrode, and instability of the Li metal anode, which typically occur in conjunction with the 'basic' reaction of the Li–O$_2$ batteries, lead to poor cyclability and low energy efficiency of the system.[6–10]
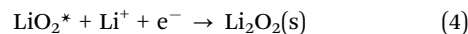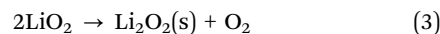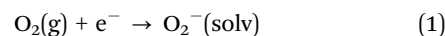
To resolve these issues and achieve significant improvement in Li–O$_2$ batteries, a fundamental understanding of the reaction mechanism is indispensable and the elucidation of the origin of these issues should be preceded. Even though Li–O$_2$ batteries are expected to operate based on simple reaction chemistry, the formation of reactive intermediates during cycling can drive various types of additional chemical reactions.[10–12] Moreover, recent studies have shown that the discharge/charge reaction can be greatly altered even by a small change in the electrolyte, catalyst, or constituting materials of the air electrode, which also results in notably different electrochemical properties.[8,13–15] Although our understanding of the reaction mechanism has progressed and been clarified with these recent important observations and proposed mechanisms, some of the reports are conflicting. Thus, a more comprehensive picture of the interplay among the cell components and its relation to the discharge/charge reaction is needed. A timely update on the findings concerning the fundamental reaction mechanism is becoming more critical in this rapidly emerging Li–O$_2$ battery field. In this progress report, we therefore carefully review the most recent discoveries concerning the Li–O$_2$ chemistry as well as the key factors affecting its reactions during each discharge and charge process. We will focus on the mechanistic studies, rather than engineering aspects such as cell configuration and

*Kisuk Kang is a professor of materials science and engineering at Seoul National University (SNU), where he also received his BSc He did a PhD and postdoctoral studies at the Massachusetts Institute of Technology. Since 2013 he has been a tenured professor at SNU. His research laboratory focuses on developing new materials for Li ion batteries and post-Li battery chemistries—such as Na, Mg, and metal–air batteries—using combined experiments and ab initio calculations.*

**Kisuk Kang**

cathode morphology design, of which progresses are well summarized in recent elaborate review papers.[16–18]

# Reaction chemistries for discharge

## Basic formation reaction of the discharge product, Li$_2$O$_2$

The ideal operation of Li–O$_2$ batteries is based on the electro-chemical formation (discharge) and decomposition (charge) of lithium peroxide (Li$_2$O$_2$). During discharge, oxygen dissolved from the ambient air and Li ions in the electrolyte react to form LiO$_2$ and subsequently Li$_2$O$_2$ as follows.[1,2]

$$O_2(g) + e^- \rightarrow O_2^-(solv) \tag{1}$$

$$Li^+(solv) + O_2^- \rightarrow LiO_2 \tag{2}$$

$$2LiO_2 \rightarrow Li_2O_2(s) + O_2 \tag{3}$$

$$LiO_2^* + Li^+ + e^- \rightarrow Li_2O_2(s) \tag{4}$$

At the beginning of the discharge, oxygen is reduced on the electrode (1) and successively combines with a Li ion in the electrolyte, forming the metastable LiO$_2$ (2). LiO$_2$ may subsequently undergo two different reaction pathways: either a chemical disproportionation involving two LiO$_2$ molecules (3) or a continuous electrochemical reduction of LiO$_2^*$ (* refers to species adsorbed on the electrode surface) with an additional electron and Li ion (4), both of which result in the formation of Li$_2$O$_2$. The kinetics of each reaction step and the stability of the intermediates are greatly affected by the surrounding conditions, leading to distinct electrochemical properties, including specific capacity, rate capability, and energy efficiency.[14,19–22] Accordingly, recent attention has been paid to providing a better understanding of the effect of the surroundings, which will be specifically discussed in the following sections.

## Parasitic reactions involving the electrolyte and its stability

An oxygen radical (O$_2^-$) is produced during the discharge process, and such a highly reactive species can react with the surrounding electrolyte, consuming the electrolyte and resulting in a parasitic reaction. The degradation of the electrolyte may occur *via* nucleophilic attack of the O$_2^-$ on the carbon atom of the solvent molecule or H-abstraction.[11,12,23] Because O$_2^-$ is a strong nucleophile, it is prone to attack the electron-deficient part of the solvent (*i.e.*, carbon atom), forming a [solvent–O$_2$]$^-$ complex, which subsequently follows a highly exergonic decomposition reaction.[11,12,24] In this respect, it has been suggested that the stability of solvents can be predicted from the formation energy of the initial [solvent–O$_2$]$^-$ complex ($\Delta G_r$) and its reaction barrier ($\Delta G_{act}$).[11,12,24] From the theoretical calculations of $\Delta G_r$ and $\Delta G_{act}$ for various solvents combined with cyclic voltammetry (CV) experiments, it was proposed that solvents with $\Delta G_{act} > 24$ kcal mol$^{-1}$ were stable in the CV test, whereas solvents with both $\Delta G_{act}$ and $\Delta G_r$ less than 20 kcal mol$^{-1}$ were not.[11,24] Carbonate-based electrolytes such as ethylene carbonate, propylene carbonate, and dimethyl carbonate, which were used in the early development of Li–O$_2$ batteries, were predicted to be vulnerable to nucleophilic attack ($\Delta G_{act}$ and $\Delta G_r < 20$ kcal mol$^{-1}$)

**Table 1** Calculated reaction energies ($\Delta G_r$) and activation energies ($\Delta G_{act}$) of initial complex formation (ICF), $pK_a$, donor number (DN) and acceptor number (AN) of representative electrolytes used in Li–O$_2$ batteries

| | $\Delta G_r$ (kcal mol$^{-1}$) | $\Delta G_{act}$ (kcal mol$^{-1}$) | $pK_a$ in DMSO | Donor number (DN) (kcal mol$^{-1}$) | Acceptor number (AN) (kcal mol$^{-1}$) |
|---|---|---|---|---|---|
| Ethylene carbonate (EC) | −6.94 [11] | 14.22 [11] | — | 16.4 [25] | — |
| Propylene carbonate (PC) | −5.64 [11] | 15.47 [11] | — | 15.1 [23] | 18.3 [23] |
| Dimethyl carbonate (DMC) | −11.39 [11] | 12.42 [11] | — | 17.2 [25] | — |
| Dimethoxy ethane (DME) | 19.88 [11] | 31.56 [11] | 51.8 [23] | 20.0 [19] | 10.2 [19] |
| Tetraethylene glycol dimethyl ether (TEGDME) | — | — | — | 16.6 [27] | 11.7 [27] |
| Dimethyl acetamide (DMA) | 19.45 [24] | 37.36 [24] | 34.4 [23] | 27.8 [19] | 13.6 [19] |
| Dimethyl sulfoxide (DMSO) | 3.8 [26] | 21.6 [26] | 35.1 [23] | 29.8 [19] | 19.3 [19] |
| Acetonitrile (MeCN) | 18.96 [11] | 24.92 [11] | 31.3 [19] | 14.1 [19] | 18.9 [19] |

by the oxygen radicals, which is consistent with experimental findings.[10–12] Table 1[11,19,23–27] summarizes key properties of representative solvents which are indicative of the relative stability against the oxygen radicals. Li–O$_2$ cells using carbonate-based electrolytes yield byproducts such as Li$_2$CO$_3$, LiOH, and HCO$_2$Li instead of Li$_2$O$_2$ (reaction (1) in Fig. 1). Alternatively, to avoid such side reactions, solvents with relatively high $\Delta G_r$ and $\Delta G_{act}$, e.g., ether-, sulfone-, and amide-based solvents, have been adopted, which has succeeded in predominantly yielding Li$_2$O$_2$ (reaction (2) in Fig. 1).[28–30]

Even for the suggested non-carbonate-based electrolytes, electrolyte degradation can still occur via the acid–base reaction between O$_2^-$ and a solvent molecule, as O$_2^-$ is known as a strong base:[24,31–33] HA + O$_2^-$ → A$^-$ + HO$_2$, where HA represents the solvent molecule. This process can also be interpreted as nucleophilic attack of O$_2^-$ to the hydrogen atom of the solvent molecule, i.e., H-abstraction. The formation of HO$_2$ as well as A$^-$ eventually results in decomposition of the electrolyte and the formation of byproducts (reaction (3) in Fig. 1).[19,23,24,34] Because of the nature of the acid–base reaction, the acidity of the solvent and concentration of O$_2^-$ can be considered key descriptors of the reactivity. A solvent molecule with weak acidity, i.e., a high $pK_a$, can strongly resist H-abstraction from

oxygen radicals. However, a solvent molecule with a low $pK_a$ remains vulnerable to H-abstraction. The concentration of O$_2^-$, another important key descriptor, can be affected by properties of the electrolyte solvent, such as its solvating capability. Solvents with a low donor number (DN) and low acceptor number (AN), which generally exhibit weak solvating ability, induce a low concentration of O$_2^-$, thus possibly suppressing the H-abstraction. Solvents with high $pK_a$ and low AN and DN, such as dimethoxyethane (DME), have been reported to be stable against oxygen radicals for over one week.[19,23,24] (See Table 1) Nevertheless, repeated cycles still make them unstable, degrading the efficiency of the Li–O$_2$ cells.[9,35] The identification of a new electrolyte that exhibits high stability against the nucleophilic attack of oxygen radicals remains challenging and is indispensable for the realization of long-life Li–O$_2$ batteries. In parallel, the exploration of additive materials in the electrolyte, which can capture and stabilize reactive oxygen radicals, can be an alternative plausible solution, as developing an intrinsically stable electrolyte can be a daunting task.

### Electrolytes altering the basic discharge mechanism

The stability of the intermediate discharge product is sensitively affected by the properties of the electrolyte, which also affects the formation mechanism of the final discharge product.[13,36–42]
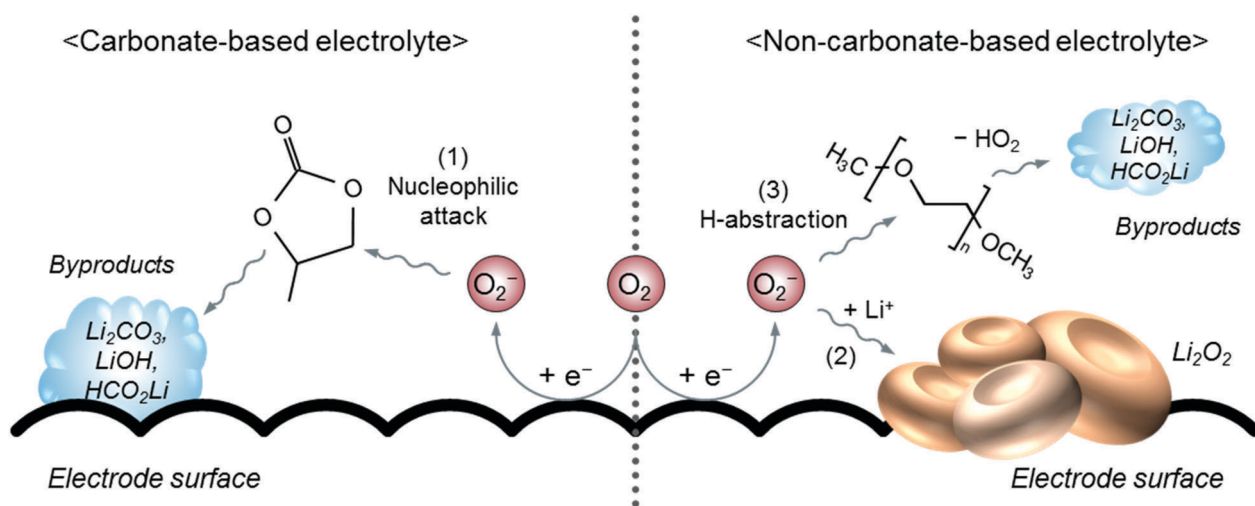


**Fig. 1** Schematic illustration of possible discharge reactions involving oxygen radicals in different electrolyte systems. (1) Nucleophilic attack of an oxygen radical in a carbonate-based electrolyte and the subsequently produced byproducts. (2) Reaction between oxygen radicals and Li ions to produce Li$_2$O$_2$ in a non-carbonate-based electrolyte. (3) H-abstraction reaction induced by oxygen radicals and the subsequently produced byproducts in a non-carbonate-based electrolyte.

Recent studies have proposed two models for the $O_2$ reduction process. One involves the formation of toroidal $Li_2O_2$ particles grown from the intermediate $LiO_2$ phase through chemical disproportionation (3), and the other describes the formation of film-like $Li_2O_2$ on the electrode surface (4).[13,43,44] The two different models for $Li_2O_2$ formation can be understood based on a simple physical parameter: DN of the electrolyte. In a previous report, reduction processes of $O_2$ during discharge were comparatively investigated in four solvents with a range of DN values (1-methylimidazole (Me-IM): 47, dimethyl sulfoxide (DMSO): 30, DME: 20, acetonitrile (MeCN): 14).[13] It was suggested that the high-DN solvents (Me-IM, DMSO) can strongly solvate and stabilize $Li^+$ or $Li^+$-containing intermediate species such as $LiO_2$ in the electrolytes. The strong solvation stabilizes the soluble $LiO_2$ in the electrolyte, which allows the disproportionation of $LiO_2$ to occur stably in the solution, accompanying the growth of $Li_2O_2$ particles. This solution-mediated growth mechanism will result in continuous precipitation, yielding relatively large $Li_2O_2$ particles as shown in Fig. 2a (right). In contrast, the low-DN solvents (DME, MeCN) exhibited much weaker solvation capability; therefore, the intermediate $LiO_2^*$ cannot be stably liberated into the electrolyte from the electrode surface where it is generated.

The primary population of $LiO_2^*$ on the surface of the electrode and its instability lead to a surface-driven growth mechanism (4), where a fast second reduction to $Li_2O_2$ generally occurs on the electrode surface, depositing a thin layer of discharge product as shown in Fig. 2a (left).

Notably, these two mechanisms can result in remarkably distinct morphologies and properties of the $Li_2O_2$ discharge product.[13] The surface-driven mechanism in the low-DN solvents generally induces film-like $Li_2O_2$ formation on the surface of the electrode. In contrast, the precipitation of $Li_2O_2$ particles in the solution-mediated mechanism leads to particles with a large toroidal shape for the high-DN solvents.[13,30,44] Note that the crystallinity of the film-like $Li_2O_2$ is poorer than that with the toroidal morphology.[45,46] This finding is attributed to the shorter lifetime of $LiO_2^*$ adsorbed on the electrode surface and a rapid second reduction to $Li_2O_2$, which prohibit the formation of the highly crystalline phase. Moreover, the amount of discharge product, i.e., the specific capacity of the Li–$O_2$ batteries, is correlated with the morphological difference of the two. As observed in Fig. 2a (left), the specific capacity is generally lower in the low-DN electrolytes. The formation of the insulating $Li_2O_2$ film on the surface easily passivates the active
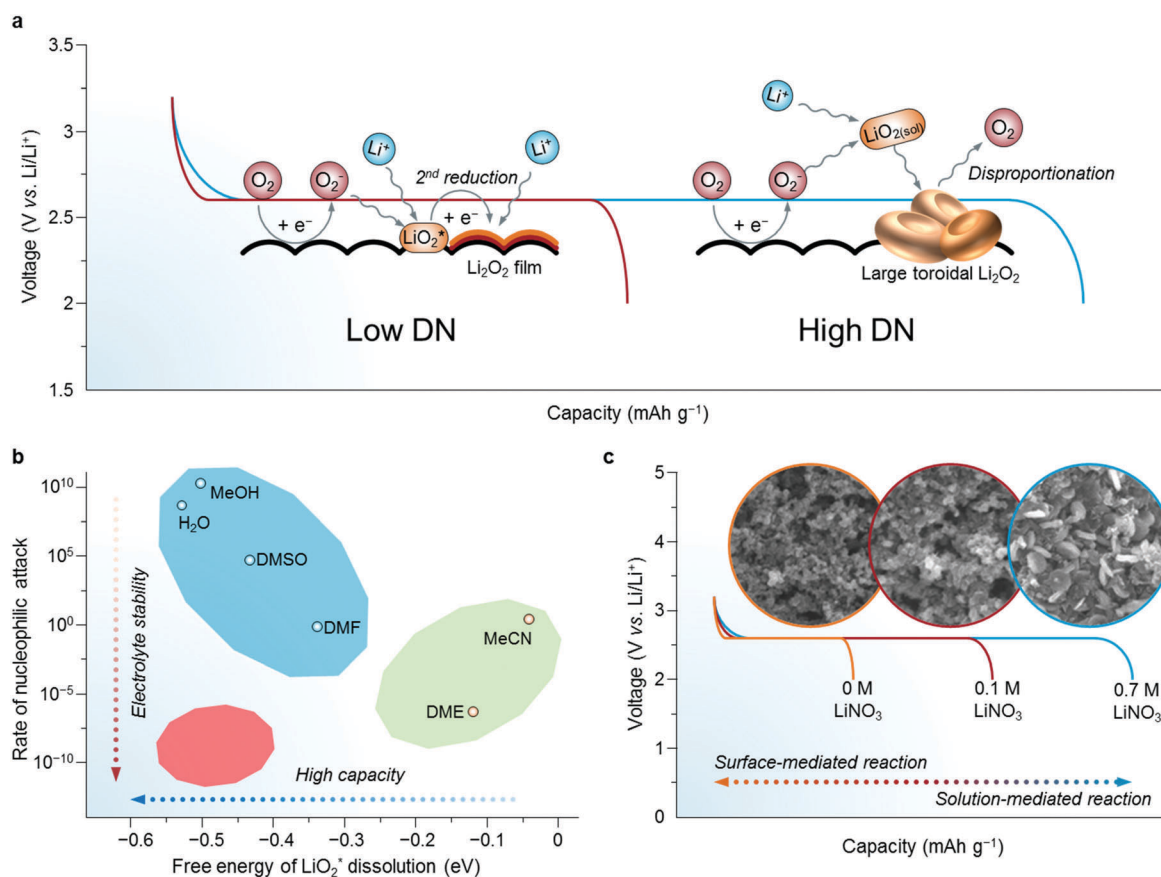


Fig. 2 Role of electrolyte solvating ability in the discharge mechanism of Li–$O_2$ batteries. (a) Schematic of discharge mechanisms in different solvents with high and low DN. (b) Relationship between the free energy of $LiO_2^*$ dissolution and the rate of nucleophilic attack of $O_2^-$ for the reported solvents. The free energy of $LiO_2^*$ dissolution represents the solvation ability of the solvent, whereas the nucleophilic attack rate represents instability against H-abstraction (ref. 19). (c) Galvanostatic discharge profiles and SEM images of Li–$O_2$ batteries for different $LiNO_3$ concentrations. Reproduced with permission. (SEM images, ref. 14) Copyright 2015, National Academy of Sciences.

2876 | Chem. Soc. Rev., 2017, 46, 2873–2888

This journal is © The Royal Society of Chemistry 2017

electrode surface, which rapidly increases the cell resistance with the progress of the discharge, thus reducing the total capacity. However, the solution-mediated $Li_2O_2$ growth in high-DN electrolytes, which generates large toroidal particles, results in a much higher specific capacity in Li–$O_2$ batteries (Fig. 2a (right)). Less tendency to passivate the fresh electrode surface aids in the continuing electrochemical reaction on the electrode. However, it should be noted that the high-DN solvent is not always an optimal choice for Li–$O_2$ batteries because there are fundamental trade-offs between the capacity and electrolyte stability.[19] Although high-DN solvents can increase the discharge capacity by triggering the solution-mediated growth of $Li_2O_2$, a solvent with high DN is vulnerable to H-abstraction because of the high concentration of $O_2^-$, as discussed above, which results in solvent degradation.[19,23] Fig. 2b presents a schematic diagram that plots the stability of a solvent against H-abstraction reaction (rate of nucleophilic attack) vs. the tendency to drive solution-mediated $Li_2O_2$ growth ($LiO_2^*$ dissolution energy), which was recently described by Khetan et al.[19] There is an inverse correlation between the two competing effects: solvents with stronger solvating properties are relatively unstable to the H-abstraction reaction (blue region), whereas solvents with better stability against H-abstraction exhibit relatively poor $LiO_2^*$ solvating properties (green region), thus exhibiting reduced discharge capacity. As observed for the known electrolyte systems in Fig. 2b, selecting an appropriate electrolyte with both good solvating properties (higher capacity) and stability (better cycle stability) remains challenging, which suggests that the electrolyte systems in the red region should be explored.

On the other hand, in Na–$O_2$ battery fields, it was recently suggested that the solvation ability has a greater influence on the $NaO_2$ growth mechanism than the solvent's DN properties.[21] While strong solvent–solute interactions between the Na ion and TEGDME produce submicrometric crystallite $NaO_2$ on carbon surfaces, DME, which has a weak solvation ability compared to TEGDME, could promote cubic crystal growth of ~10 micro-sized particles. The origin is that a weak interaction between solvent–solute requires a low desolvation barrier for forming $NaO_2$ products, which can lead to the crystal growth of $NaO_2$. In this system, solvation–desolvation kinetics is the major concern determining the morphology of final discharge products, instead of the DN properties of the electrolyte. Although, a fundamental understanding of the effect of solvent is still under discussion and is worthy of further study, it is a clear fact that the properties of the electrolyte are the important factors to be considered when designing Li–$O_2$ batteries.

The types of salt dissolved in the electrolyte can also affect the reaction mechanisms of Li–$O_2$ batteries. Recently, it was demonstrated that the discharge capacity could be enhanced by altering the nature of electrolytes with appropriate salt anions.[14,42] As observed in Fig. 2c, the specific capacities were systematically increased by adding lithium nitrate ($LiNO_3$) to the electrolyte; the cell with 0.7 M $LiNO_3$ exhibits a more than four-fold increase in the specific capacity compared with that without $LiNO_3$. The addition of $LiNO_3$ also changes the morphology of the discharge products to a larger toroidal shape,

as observed in the scanning electron microscopy (SEM) images in Fig. 2c. It was claimed that the $NO_3^-$ anions in the solvents can enhance the donicity of the electrolyte, which in turn leads to increased $O_2^-$ stabilities in the solvent and triggers the solution-mediated growth mechanism of $Li_2O_2$ formation.[14] Because the reaction intermediates are coordinated with the solvent molecules and surrounded by salt ions in the electrolyte, the reaction paths are affected by their chemical properties; thus, electrolyte selection should be carefully considered in Li–$O_2$ batteries.

### Effect of water as an additive

Recent findings indicate that even a trace amount of water in the electrolyte can have a marked effect on the discharge mechanism for Li–$O_2$ batteries. In a series of reports, it was observed that the discharge capacity of Li–$O_2$ batteries could increase with the addition of water in the electrolyte.[47–50] Aetukuri et al. suggested that the addition of water in the electrolyte aids in the dissolution of $LiO_2^*$ from the electrode surface, which helps to generate large crystalline $Li_2O_2$ (Fig. 3a).[43] $H_2O$, a strong electron acceptor, in the electrolyte could stabilize $O_2^-$ and promote the dissolution of $LiO_2^*$ into the electrolyte, which sequentially allows the disproportionation reaction (3). Because the induced solution growth mechanism leads to the precipitation of large toroidal $Li_2O_2$ particles, the discharge capacities can be substantially enhanced by increasing the $H_2O$ content in the electrolyte (Fig. 3b), and toroidal particles become gradually noticeable (Fig. 3c). Similarly, other additives such as methanol and perchloric acid were demonstrated to also be capable of controlling the lifetime of $LiO_2^*$; however, their operation mechanisms remain to be further investigated.[43,49] Moreover, there is another explanation for the formation of large toroidal particles by adding water into the electrolyte. Kwabi et al., recently suggested that water decreases the $Li_2O_2$ nucleation rate at the electrode surface, which lead to the formation of large $Li_2O_2$ growth through solution-mediated growth.[50]

Notably, the Zhou group reported that an excess amount of $H_2O$ in the electrolyte yielded discharge products in disk form and not the typical toroidal shape, which was revealed to be due to the formation of LiOH.[20,51,52] They suggested that the use of electrolytic $MnO_2$ (EMD) promotes the involvement of $H_2O$ in the discharge reaction, where an excess amount of $H_2O$ reacts with the discharge product $Li_2O_2$, producing LiOH and $H_2O_2$ (5). The $H_2O_2$ is then decomposed into $H_2O$ and $1/2O_2$ with the aid of EMD (6), which triggers continuous formation of LiOH during the discharge.[20,51,52]

$$Li_2O_2(s) + 2H_2O(l) \rightarrow 2LiOH(s) + H_2O_2(l) \qquad (5)$$

$$H_2O_2(l) \rightarrow H_2O(l) + \tfrac{1}{2}O_2(g) \qquad (6)$$
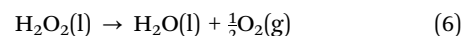
During the reaction with $H_2O$, large toroidal particles of $Li_2O_2$ are split into a layered morphology, and large sheets of LiOH are formed in the electrode (Fig. 3c). More recently, the Grey group revealed that the use of LiI together with $H_2O$ can induce the growth of large LiOH crystals and accelerate the formation of LiOH.[53] The reversible formation and decomposition of large
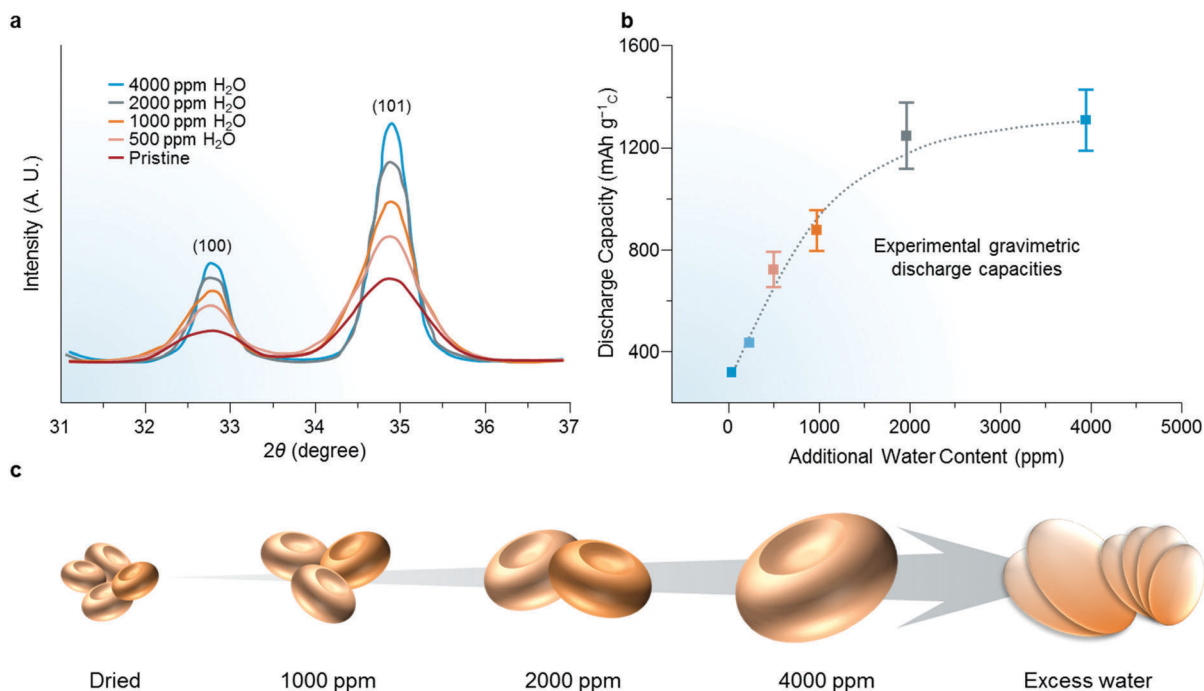
**Fig. 3** Effect of water on the discharge products of Li–O₂ batteries. (a) XRD patterns of the electrodes after discharge using 1 M lithium bis(trifluoromethane sulfonyl) imide (LiTFSI) in DME for different $H_2O$ contents (ref. 43). (b) Tendency of discharge capacities with varying $H_2O$ contents (ref. 43). (c) Schematic illustration of morphologies of $Li_2O_2$ as a function of $H_2O$ content (ref. 51).

LiOH crystals with the help of a LiI redox mediator could lead to a high specific capacity with unprecedentedly low charge/discharge overpotential. This system is worthy of further exploration in terms of both fundamental science as an alternative chemistry and practical viability. A series of studies confirms that the $H_2O$ content in the electrolyte can significantly affect the properties of the discharge products and should thus be carefully controlled in regulating the reactions in Li–O₂ batteries.

## Catalysts promoting the discharge reaction

Catalysts for discharge reactions, *i.e.*, the oxygen reduction reaction (ORR), have been relatively less studied compared with oxygen evolution reaction (OER) catalysts, which are considered to be important in reducing the charging polarization of Li–O₂ batteries, as will be discussed later in detail. However, recent studies have shown that ORR catalysts can also greatly affect the properties of discharge products of Li–O₂ batteries by affecting the morphology, crystallinity, and intermediate discharge phases, as schematically illustrated in Fig. 4.[54–56] As discussed above, $Li_2O_2$ preferentially exhibits a toroidal morphology in strongly solvating electrolytes (Fig. 4a).[57–59] However, it has been claimed that embedding certain crystalline catalysts in the electrode induces a film-like morphology on the surface of the electrode, as shown in Fig. 4b.[45,55,56,60] The reason for the different morphologies of the reaction products even in the same electrolyte was explained in terms of the oxygen affinity of the catalyst.[45,61] The surface of the catalyst can have a preferential affinity for reactive oxygen species (O₂ and LiO₂), which would delay the liberation of LiO₂* into the electrolyte.[56] The intermediate discharge phases trapped on the surface subsequently take
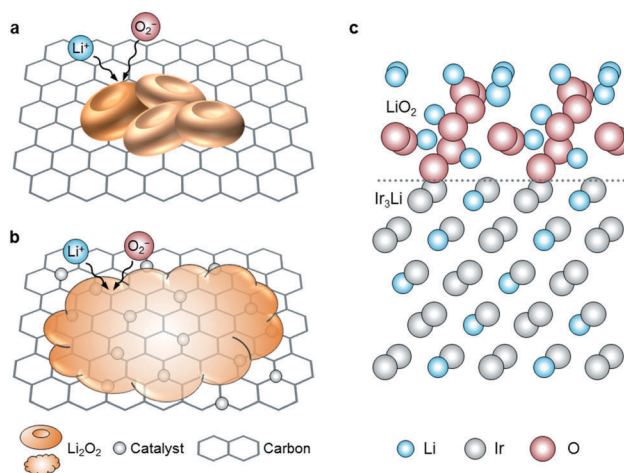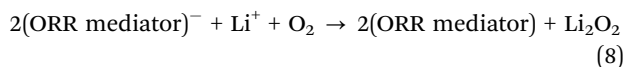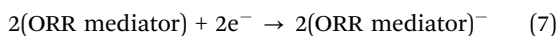


**Fig. 4** Schematic illustration of morphologies of the discharge products with and without a catalyst. (a) Toroidal-like $Li_2O_2$ forms in a strongly solvating electrolyte. (b) Use of a catalyst can induce film-like formation. (c) Epitaxial growth of the $LiO_2$ phase supported by a similar crystallographic lattice of the intermetallic compound $Ir_3Li$ (ref. 5).

additional electrons from the electrode to form film-like $Li_2O_2$ (4) instead of being dissolved into the electrolyte to follow the disproportionation reaction (3). Recently, it was also suggested that Ir-decorated reduced graphene oxides could promote the formation of a solid $LiO_2$ product, which has been known to be metastable in Li–O₂ batteries.[5] The intermetallic compound of $Ir_3Li$ formed was suspected of being capable of providing a favorable growth site for $LiO_2$ because of the similar crystallographic lattice between $LiO_2$ and $Ir_3Li$ (Fig. 4c).

Thus, the epitaxial growth of $LiO_2$ on a (121) facet of $Ir_3Li$ could enable the formation of a needle-like $LiO_2$ phase on the electrode. These findings indicate that catalysts can potentially stabilize the intermediate discharge phase by offering a platform for stable growth. This approach is effective in utilizing the metastable $LiO_2$ phase as a final discharge product and proposes a new type of Li–$O_2$ battery with an intrinsically low overpotential. However, the proposed reaction mechanism should be further verified before being considered for practical viability.

The concept of a soluble catalyst, which can be dissolved in the electrolyte (in contrast to a solid catalyst embedded in the electrode) has been recently suggested.[62,63] Such a soluble catalyst is capable of mediating the electrochemical reaction occurring in the electrolyte, thus it is also called a redox mediator. An ORR soluble catalyst can mediate the electron transfer between the electrode and oxygen in the electrolyte during the discharge. In the presence of a soluble catalyst with a higher reduction potential than that of the $O_2/O_2^-$ redox couple, the ORR mediator is reduced upon the discharge before the oxygen reduction process occurs (7). Subsequently, the reduced ORR mediator participates in the formation of $Li_2O_2$ by transferring an electron to the group of $Li^+$ and $O_2$ as described in reaction (8).[64,65]

$$2(\text{ORR mediator}) + 2e^- \rightarrow 2(\text{ORR mediator})^- \quad (7)$$

$$2(\text{ORR mediator})^- + Li^+ + O_2 \rightarrow 2(\text{ORR mediator}) + Li_2O_2 \quad (8)$$

In this case, the discharge voltage can be controlled and upshifted by selecting an ORR mediator with an appropriate redox potential. Because the reduction of the ORR mediator is the sole electrochemical reaction here, the discharge voltage of a Li–$O_2$ cell is determined by its redox potential. Matsuda *et al.* experimentally demonstrated that the discharge voltages in Li–$O_2$ batteries are determined by the average redox potentials of the used soluble catalysts.[64] In a recent paper, it was reported that 2,5-di-*tert*-butyl-1,4-benzoquinone (DBBQ) is capable of mediating the discharge reaction, exhibiting an impressively high specific capacity even when using a low-surface-area air electrode.[66] It was proposed that the DBBQ is first reduced upon the discharge and temporarily coordinates with the Li ion. Subsequently, the DBBQ–Li complex forms DBBQ–Li–$O_2$ with an oxygen molecule, which is further reduced, leading to the precipitation of the $Li_2O_2$ discharge product and liberating the DBBQ again. Interestingly, the DBBQ not only reduced the overpotential during the discharge but also triggered the solution-mediated reaction even in a weakly solvating electrolyte, highlighting the decisive role of the ORR mediator in determining the discharge mechanism. The shift of the discharge mechanism from the surface-dominated reaction to the solution-mediated reaction could result in the remarkable enhancement of the capacity regardless of the pristine electrolyte nature.

Soluble catalysts can also mediate the discharge reaction by playing the role of an oxygen carrier. It was reported that iron phthalocyanine (FePc) could shuttle oxygen to growth sites of $Li_2O_2$ by effectively absorbing the oxygen molecule at the center of FePc.[67] The Fe atom in the center of the 2D molecule of FePc

attracts the oxygen molecule dissolved in the electrolyte, forming a complex, which is reduced on the electrode during discharge $[(\text{FePc–}O_2) \rightarrow (\text{FePc–}O_2)^-]$. The complex then reacts with a Li ion to form FePc–LiOOLi and diffuses to the nucleation site, where $Li_2O_2$ discharge products are detached with the complex returning to the initial state (FePc). These soluble catalysts generally promote the solution-mediated reaction and can potentially reduce the side reaction considering that the use of a soluble catalyst reduces the exposure time of reactive oxygen radicals to the electrolyte. Although the presence of reactive oxygen radicals in the discharge process induces side reactions such as electrolyte deterioration and carbon electrode corrosion in Li–$O_2$ batteries, soluble catalysts are a promising solution to regulating oxygen radicals and are worthy of further intensive studies.

### Kinetic factors affecting discharge mechanism

In the previous discussion, we focused on mechanistic understanding of Li–$O_2$ batteries based on key parameters such as electrolyte, salt, water, and catalyst, which thermodynamically alter the discharge reaction. However, there are several kinetic issues that can affect Li–$O_2$ chemistry, which are worth further mentioning.

(1) Discharge rate: while Li–$O_2$ cells discharged at a slow current rate form a large crystalline $Li_2O_2$, cells with a fast current rate exhibit film-like formation of $Li_2O_2$ on the electrode surface. At a high current rate, seed nucleation of $Li_2O_2$ on the electrode surface is accelerated and an additional reduction reaction on the electrode surface is favoured through the reaction (4) (*i.e.*, $LiO_2^* + Li^+ + e^- \rightarrow Li_2O_2(s)$). In such a case, it tends to form surface-precipitated $Li_2O_2$ particles, which also result in a low discharge capacity. Otherwise, at a low current rate, the disproportionation of $LiO_2$ is favoured *via* the reaction (4) due to the relatively weak binding of the intermediate to the electrode surface, and it can deliver a relatively high discharge capacity.[68–70] Similar discussions were made according to the overpotential applied to an electrode. In the Li–$O_2$ cells at low overpotential, the first intermediate of $O_2^{*-}$ is formed and easily diffuses into the solution. Then, it forms large $Li_2O_2$ particles through the solution-mediated mechanism. On the other hand, at high overpotential, $LiO_2^{*-}$ may play the role of an intermediate, but it is prone to be further reduced to $Li_2O_2$ near the electrode surface, resulting in film-like formation. The formation of the first intermediates ($O_2^{*-}$ or $LiO_2^{*-}$) highly depends on the overpotential applied to the electrode, and it results in different electrochemical properties.[71]

(2) Oxygen diffusivity and solubility: the diffusivity and solubility of oxygen can affect the discharge capability of Li–$O_2$ batteries. It was demonstrated that oxygen solubility could be enhanced by increasing the salt concentration in the electrolyte.[22] It implies that the discharge capacity can be enhanced by choosing an appropriate salt and its concentration in the electrolyte. Interestingly, this could be dominantly observed in a specific electrolyte system containing large anions such as $TFSI^-$ and $FETI^-$. Meanwhile, oxygen diffusivity is particularly influenced by solvent molecule size because the diffusion of oxygen can be hindered by the large solvation sphere of solvent.

This journal is © The Royal Society of Chemistry 2017

*Chem. Soc. Rev.*, 2017, **46**, 2873–2888 | 2879

In the aspects of mass transport ability of reactants, the choice of electrolyte solvent, salt, and its concentration would be also important key parameters for Li–O₂ batteries.[22]

Although the discharge reaction of Li–O₂ batteries involves only two primary elements, Li and O, its mechanism is significantly altered with the formation and stability of reaction intermediates, which are affected by various cell parameters. Moreover, reactive intermediates can induce side-reactions with cell components, *i.e.* electrolytes,[11,12] Li metal,[72–75] and carbon air electrodes,[7,18,76] which degrades cell performance. Therefore, future research should focus on regulating the reactivity of various intermediates in each relevant reaction step.

# Reaction chemistries for charge

### Decomposition mechanism of discharge products during a charge process

The charging process of ideal Li–O₂ batteries involves the electrochemical decomposition of Li₂O₂ formed on the air electrode and should follow the reverse process of the discharge reaction of (1)–(4). However, the process is not a simple reverse reaction but can be accompanied by several metastable states that do not appear in the discharge reaction, depending on the nature of the discharge products. For a microscopic picture of the decomposition, it has been speculated that the reaction would occur primarily at the interface between the electrode and Li₂O₂, liberating lithium and oxygen as described in the green box of Fig. 5a. Several *in situ* studies[77,78] have confirmed the decomposition of Li₂O₂ occurring at the electrode/Li₂O₂ interface by the formation of void spaces at the interface during the charge. Researchers have suggested that the void could be successively filled by the collapse of Li₂O₂ particles during the charge; therefore, even large Li₂O₂ particles could be decomposed.[78] However, the decomposition would also occur at the interface between Li₂O₂ and the electrolyte, where Li ions and oxygen gas can be easily released from the Li₂O₂ surface if charge carriers can be transferred through the particle of Li₂O₂ (blue box in Fig. 5a). Indeed, Zheng *et al.* claimed that the decomposition of Li₂O₂ occurs mainly at the interface with the electrolyte based on *in situ* environmental SEM experiments,[79] which contradicted previous transmission electron microscopy measurements.[77] However, crystalline Li₂O₂ is known to be electrically insulating, and, in this case, it would be difficult to expect the charge transfer to occur sufficiently fast for the decomposition of large particles of Li₂O₂.[80–84] Moreover, according to theoretical calculations of the transition state of crystalline Li₂O₂ decomposition, the overpotential of releasing Li ions and O₂ gas at the Li₂O₂ surface is estimated to be small (<0.2 V) in the absence of the electric charge transport limitation,[85–87] whereas much higher charging overpotential (>1.5 V) has been experimentally reported in Li–O₂ cells.[1,9,88,89] These findings imply that the electrical charge transport issue in Li₂O₂ would not be a negligible factor and that the nature of the electrochemically formed Li₂O₂ should be carefully considered.[40,77,90]
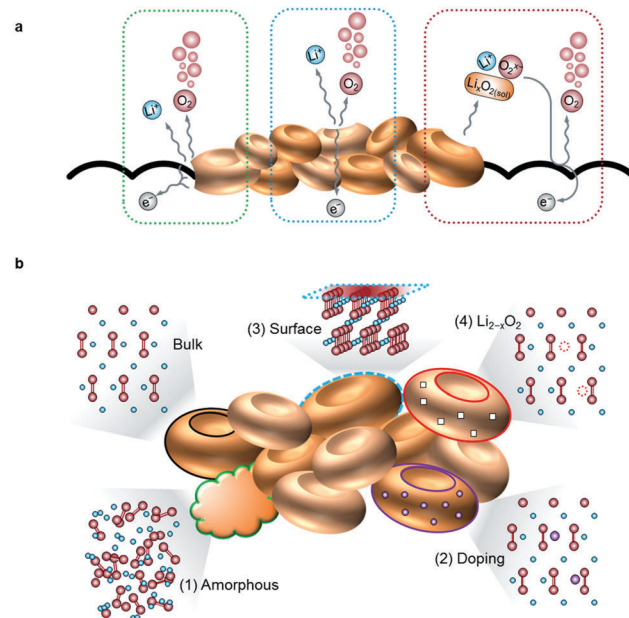


Fig. 5 Reaction sites of Li₂O₂ decomposition and various atomic structures of Li₂O₂. (a) Possible reaction sites for electrochemical decomposition of Li₂O₂, *i.e.*, electrode/Li₂O₂, Li₂O₂/electrolyte, and electrode/electrolyte interfaces. (b) Atomic structures of the reported defects in Li₂O₂, which can enhance the electronic/ionic conductivities. Oxygen, lithium, and metal dopant elements are designated as red, blue, and purple balls, respectively.

Unlike the direct decomposition of Li₂O₂, the species of LiO₂ or Li⁺–O₂⁻/²⁻ ion pairs, which are dissolved from the Li₂O₂ into the electrolyte, if any, can be electrochemically decomposed at the electrode/electrolyte interface (red box in Fig. 5a).[19,43,91] However, this type of charge process is believed to be less dominant because of the unfavorable dissolution energy of Li₂O₂ to produce LiO₂ or Li⁺–O₂⁻/²⁻ ion pairs.[80,92] Note that this process contrasts with that for Na–O₂ batteries, which undergo a dissolution and solution-mediated charging process because of the relatively high solubility of NaO₂ in the solvents.[93–95] It is expected that the three types of decomposition reactions in Fig. 5 would occur simultaneously during the charge. However, the major charging reaction mechanism would be determined by how the charge carriers are transferred through Li₂O₂ particles, which would be affected by the prior discharge process and their dissolution properties in the electrolyte.

### Charge transport nature in Li₂O₂

The structure of electrochemically formed Li₂O₂ has been frequently observed to display a significant defective characteristic compared with commercial Li₂O₂ crystalline powder based on X-ray diffraction (XRD),[96–99] X-ray absorption near-edge structure (XANES) analysis,[98] and Raman spectroscopy.[100] These findings imply that the defect structure of Li₂O₂ is of critical importance in understanding the charge transport properties of the Li₂O₂ discharge product. A theoretical study revealed that the ionic and electronic conductivities of crystalline Li₂O₂ were ~10⁻¹⁹ S cm⁻¹,[81] which is extremely low for normal electronic/ionic conduction. However, successive studies reported that

2880 | *Chem. Soc. Rev.*, 2017, **46**, 2873–2888

This journal is © The Royal Society of Chemistry 2017

defects in $Li_2O_2$ could significantly increase the conductivity of $Li_2O_2$, if present. Fig. 5b presents a schematic illustration of four representative defect scenarios, which may occur in electrochemically induced $Li_2O_2$. One of the possible scenarios is the formation of a disordered $Li_2O_2$ phase ((1) in Fig. 5b). Because the discharge process of Li–O$_2$ batteries occurs at room temperature, an amorphous $Li_2O_2$ phase is usually observed experimentally.[45,70,101,102] The ionic and electronic conductivity of the amorphous $Li_2O_2$ were predicted to be $10^{-7}$ and $10^{-16}$ S cm$^{-1}$, respectively, which are considerably high compared with those of crystalline $Li_2O_2$.[103] Another possible scenario for the defects is the presence of heteroatoms in $Li_2O_2$, as observed in (2) of Fig. 5b. When a metal oxide catalyst is in contact with a $Li_2O_2$ particle, for example, transition metals can be doped in $Li_2O_2$, inducing defects in $Li_2O_2$. In a case study of Co doping, Radin et al. claimed that the ionic and electronic conductivities can increase by 10 orders of magnitude ($\sim 10^{-9}$ S cm$^{-1}$).[104] The surfaces of the crystal are, in principle, also intrinsic defects and can be considered to be a possible defect scenario of $Li_2O_2$ ((3) of Fig. 5b). Radin et al. performed electronic structure calculations of the $Li_2O_2$ surface and claimed that the surface of $Li_2O_2$ is metallic.[105] This finding implies that reducing the size of the discharge product may promote the charge transport kinetics in Li–O$_2$ cells; additional experimental verification should be performed.

A lithium deficiency in $Li_2O_2$, i.e., $Li_{2-x}O_2$ ((4) in Fig. 5b), is one of the most frequently observed defects in electrochemically formed $Li_2O_2$.[91,96,106] The presence of superoxide ($O_2^-$) ions was experimentally confirmed based on the characteristic signals of XANES[98] and Raman spectroscopy.[100] Considering that the charge of a Li vacancy is compensated by the $O_2^{2-}/O_2^-$ transition, the observation of a superoxide ion indicates the formation of lithium vacant sites in $Li_2O_2$. The presence of a lithium deficiency in $Li_2O_2$ has also been suggested by theoretical studies. Free energy calculations by Kang et al. revealed that the solid-solution $Li_{2-x}O_2$ phase ($0 < x < 1$) can be generated with a small overpotential of $\sim 0.3$ V[106] and that the $Li_{1.5}O_2$ ($x = 0.5$) phase becomes more stable than $Li_2O_2$ on the nanometer scale.[107] Furthermore, the lithium-deficient phases were predicted to be metallic from density of states calculations,[108] indicating that the formation of $Li_{2-x}O_2$ can also increase the conductivity of the discharge product. The presence of various forms of defects in $Li_2O_2$ can significantly affect the charge transport properties of $Li_2O_2$ and are thus suggested as important factors to consider in the decomposition reaction of the discharge product in Li–O$_2$ batteries.

## Proposed decomposition mechanisms for different types of lithium peroxides

Two distinctive charging mechanisms have been proposed in elucidating the decomposition reaction of $Li_2O_2$ in terms of the morphology, i.e., toroidal $Li_2O_2$ and film-like $Li_2O_2$.[84,91,106] Fig. 6a displays the typical charge profile of Li–O$_2$ batteries containing a toroidal $Li_2O_2$ discharge product. Even though the toroidal growth of $Li_2O_2$ benefits the specific capacity of the Li–O$_2$ cells, charge transport through the large toroidal $Li_2O_2$ particles hardly occurs because of the poor electronic conductivity of $Li_2O_2$.[13,66,81,103] Thus, it has been suggested that the charging reaction of the large toroidal $Li_2O_2$ particles would be triggered by the formation of the conductive $Li_{2-x}O_2$.[91,106] During the initial charge process (region 1), Li ions diffuse out from the crystal structure of $Li_2O_2$ with the extraction of electrons, forming the lithium-deficient intermediate phase $Li_{2-x}O_2$. After the formation of the relatively conductive $Li_{2-x}O_2$, the oxidation of $Li_{2-x}O_2$ can be expedited, evolving Li ions and oxygen gas and showing a flat voltage (region 2). This stage is followed by the decomposition of residual byproducts such as $Li_2CO_3$ at a higher potential (region 3). This mechanism has been supported by several theoretical and experimental studies.[91,96,106,109] A first-principles study by Kang et al. demonstrated that the topotactic delithiation of $Li_2O_2$ with the formation of $Li_{2-x}O_2$ is kinetically preferred to the thermodynamic equilibrium path.[106] Potentiostatic and galvanostatic intermittent titration techniques[91,109] revealed the diffusion-dominated process during the initial charging process (region 1) with a low overpotential, which is consistent with the formation of $Li_{2-x}O_2$. Furthermore, an experimental study using operando XRD confirmed the presence of sub-stoichiometric $Li_{2-x}O_2$ during the charging stage.[96] The successive operando XRD studies revealed that the electrochemically synthesized $Li_{2-x}O_2$ phase showed a faster decomposition rate than a commercial $Li_2O_2$ powder case, which implies faster charge transport and facile decomposition of electrochemically grown $Li_{2-x}O_2$.[110,111]

Fig. 6b describes a slightly different decomposition mechanism proposed for $Li_2O_2$ with film-like morphology distinguished from that of the toroidal $Li_2O_2$. According to a few theoretical studies, charge transport can occur via electron tunneling through the film, which has a thickness of less than approximately 5 nm.[84,90] The typical thickness of the $Li_2O_2$ film on a carbon air electrode has been experimentally determined to be in the range of a few nanometers.[45,55,60] In addition, the film-like $Li_2O_2$ generally exhibits a quasi-amorphous nature compared with the crystalline toroidal morphology, which implies that more facile charge conduction might occur for the film-like $Li_2O_2$ discharge product. Because of the fast electron tunneling through the relatively conductive amorphous $Li_2O_2$ film, the electrochemical decomposition of $Li_2O_2$ is more facile, and the OER polarization can become smaller compared to that for the toroidal $Li_2O_2$, as shown in Fig. 6b. This finding is consistent with previous experimental studies.[70,112] It is also observed that chemically synthesized amorphous $Li_2O_2$ exhibits 2–3 orders of magnitude higher electronic and ionic conductivity than that of crystalline $Li_2O_2$,[113,114] resulting in a relatively low charge plateau at $\sim 3.54$ V compared to the charge voltage of 3.82 V and 4.04 V obtained for annealed crystalline and commercial lithium peroxide, respectively.[114] The observed low overpotential can also be attributed to the larger contact area between the electrode and film-like $Li_2O_2$, which can promote the OER kinetics. Nevertheless, it is noted that the large contact area between $Li_2O_2$ and the carbon air electrode can easily trigger the side reaction toward the formation of $Li_2CO_3$, which is detrimental to the coulombic efficiency.[7,115] Consequently,
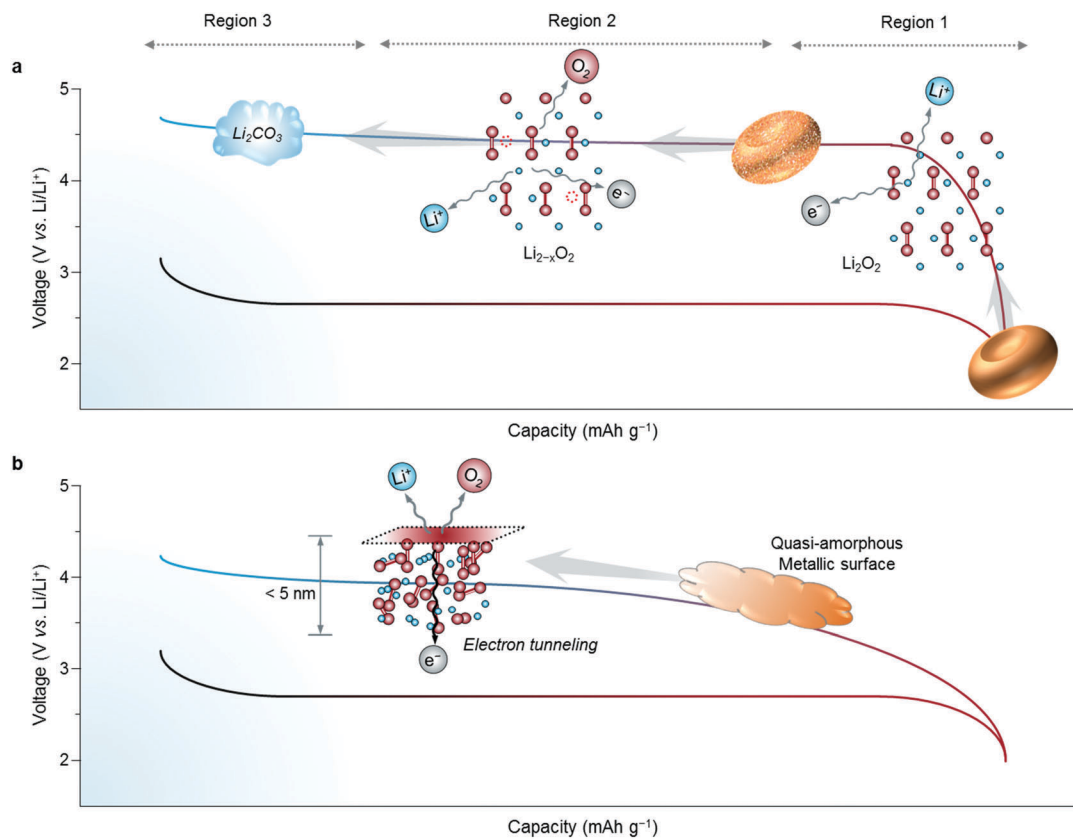
**Fig. 6** Schematic illustrations of charge profiles for Li–O₂ batteries. Inset schematics depict structural changes of Li₂O₂ during charge. (a) Charge profile of the toroid Li₂O₂ consisting of three regions: the formation of a lithium-deficient phase Li₂₋ₓO₂ (region 1), its continuous oxidation reaction (region 2), and decomposition of byproducts (region 3). (b) Charge profile of the film-like Li₂O₂ describing the decomposition of Li₂O₂ through direct electron conduction.

fast electron tunneling though film-like Li$_2$O$_2$ can be beneficial in terms of the charge overpotential; however, demerits of the thin-film morphology such as the low discharge capacity and high risk of side reactions should be considered. Since there must be trade-offs in increasing discharge capacity with toroidal Li$_2$O$_2$ and facilitating charge processes through film-like Li$_2$O$_2$, an alternative route for Li–O$_2$ chemistry which can decouple energy density and efficiency should be necessary, and the discovery of appropriate catalysts has thus been intensively studied to achieve these goals, the mechanism of which will be discussed in the following sections.

**Catalysts for oxygen evolution reactions**

OER catalysts are of critical importance in reducing the charging overpotential and have thus been extensively studied since the early developments of rechargeable Li–O$_2$ batteries.[116–121] Catalysts for OER have often been adopted from the well-known catalysts in fuel cells and water splitting, *i.e.*, noble metal and metal oxide catalysts. Even though some of these catalysts could decrease the charging overpotential, a clear description of their role has not been established.[116,117] Moreover, many researchers now argue that the classical role of catalysts appears to be negligible in Li–O$_2$ batteries[45,55,57,60,92,104,122–124] because of the significant side reactions triggered by the

catalysts and the limited solid–solid interface between Li$_2$O$_2$ and the catalyst.

Regarding noble-metal catalysts that displayed low overpotential with significant evidence of enhanced Li$_2$O$_2$ decomposition capability, it was claimed that the enhancement stems from the strong oxygen affinity of the noble metal, which can induce the film-like formation of Li$_2$O$_2$ by absorbing oxygen near the surface of the electrode during the discharge.[45,55,60] The film formation enables facile electron transport through the discharge product, as discussed above, which is regarded as the origin of the low overpotential in the decomposition reaction.[45,55] Some researchers believe that the catalytic effect can be simply attributed to the high electronic conductivity of the noble metal itself. The high electronic conductivity of metal catalysts can reduce the overall resistance of the air electrode embedding the catalysts, resulting in a small IR polarization and subsequently low overpotential.[60] Another recent claim is that noble metal catalysts can cause the formation of intermediate solution products from the electrolyte decomposition. The solution products were expected to act as a soluble catalyst, oxidizing Li$_2$O$_2$ with a low overpotential.[123,124] However, this hypothesis was recently refuted. Wang *et al.* showed that the noble metal catalyst (*i.e.*, Ru) remained active even in all-solid-state Li–O$_2$ cells, which do not contain liquid electrolytes for the mediating species.

Alternatively, it was proposed that the metal catalysts induce the formation of a lithium-deficient $Li_2O_2$ discharge product $(Li_{2-x}O_2)$.[92] Similarly, kinetic Monte Carlo simulation predicts the formation of an amorphous $Li_2O_2$ phase when a metal catalyst is present in the cell.[125] As discussed above, the defective $Li_2O_2$ exhibits better transport properties than the crystalline phase and can thus be beneficial for the decomposition reaction. Moreover, Song et al. recently suggested that the metal catalyst can promote the decomposition of by-product $Li_2CO_3$, which significantly passivates the air electrode, resulting in improved cycle life.[126] While all of the feasible mechanisms are suspected to be related to the discharging reaction rather than the charging process, the precise role of metal catalysts for Li–O$_2$ batteries remains elusive.

Metal oxides have also often been demonstrated as OER catalysts, and several catalytic mechanisms have been proposed. Yao et al. suggested that $Li_2O_2$ decomposition could be mediated via a chemical conversion reaction between $Li_2O_2$ and metal oxides, forming an intermediate $Li_xM_yO_z$ phase.[122] In this case, the faster kinetics of the charging reaction of $Li_xM_yO_z \rightarrow Li^+ + M_cO_d + O_2$ dominates over the reaction of $Li_2O_2 \rightarrow Li^+ + O_2$, thus reducing the charging overpotential. However, a few theoretical studies have claimed that metal oxides, such as $Co_3O_4$, can induce Li vacancies through $Co^{3+}$ doping in $Li_2O_2$.[104,127] The increased defect concentration is expected to improve the ionic

conductivity of $Li_2O_2$,[104] which leads to the reduced charging polarization. Even though extensive research has been conducted to elucidate the role of conventional solid-state catalysts, the operating mechanism remains vague and controversial in Li–O$_2$ batteries. Moreover, metal/metal oxide catalysts are reported to also promote electrolyte decomposition.[57,128,129] This finding implies that even if solid catalysts can improve the energy efficiency of Li–O$_2$ cells, they may simultaneously degrade the overall cell performance.

Recent interest has been focused more on soluble OER catalysts or OER mediators, which can promote the decomposition of $Li_2O_2$ by mediating the oxidation reaction in the electrolyte, as schematically depicted in Fig. 7a.[62,63] In a conventional charging reaction, the charge transport should occur through the insulating media of $Li_2O_2$, which generally induces a substantial kinetic limitation. However, with the use of an OER mediator, the charge transfer through $Li_2O_2$ is no longer necessary. Instead, the OER mediator can mediate the electron transfer between the electrode and discharge product, which leads to a facile route of decomposing $Li_2O_2$ with a significantly reduced polarization (Fig. 7a). In addition, the freely diffusible OER mediator can easily access the solid discharge product through the electrolyte; thus, even the discharge product, which is electrically isolated from the electrode, can be effectively decomposed and contribute to the charging capacity. The operation
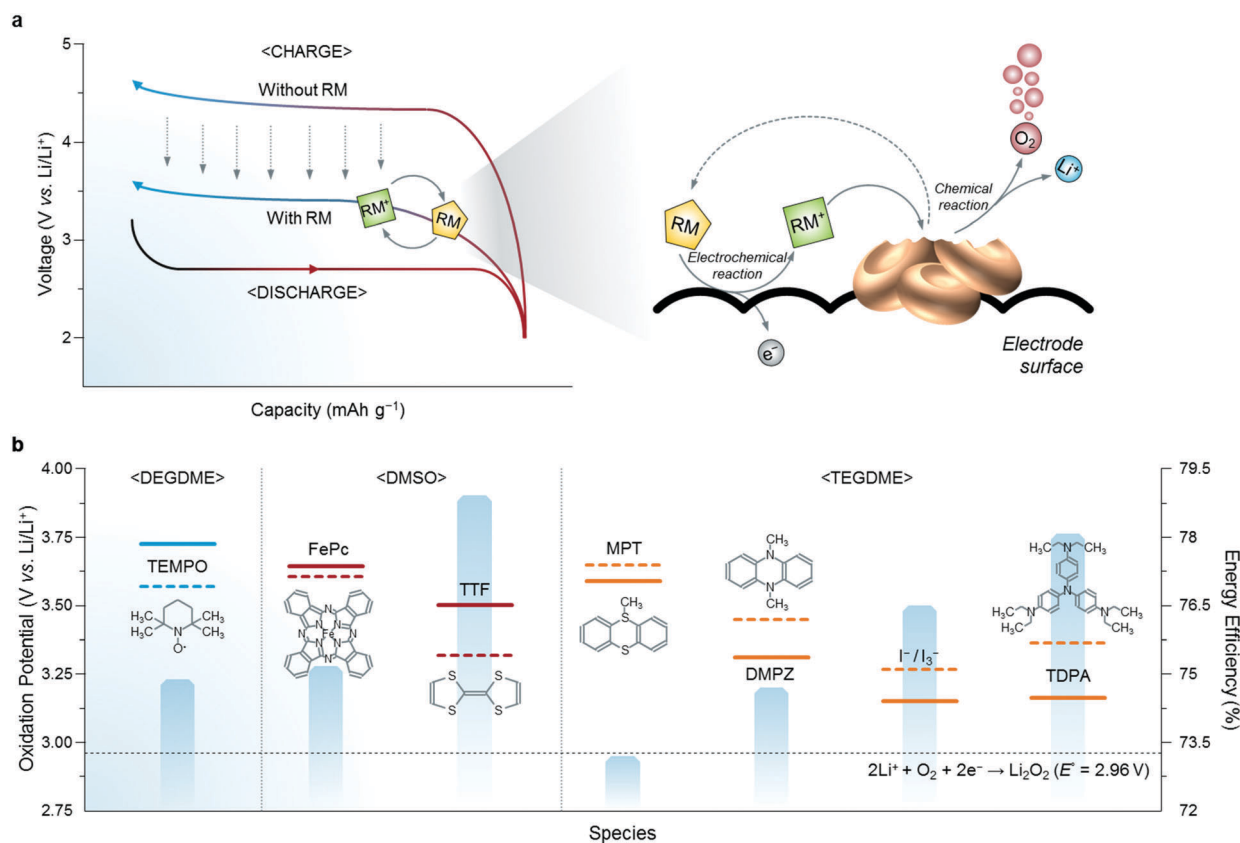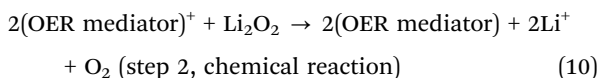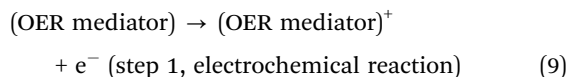


Fig. 7 Mechanism of OER mediator and comparison of the potential of OER mediators. (a) The mechanism of a soluble catalyst in the decomposition of $Li_2O_2$. (b) Comparison of the oxidation potentials (solid lines) of reported OER mediators obtained based on CV data and the average charging voltages (dotted lines) of Li–O$_2$ cells adopting each OER mediator. The bar graphs represent the energy efficiencies of Li–O$_2$ cells adopting each OER mediator.

mechanism of the OER mediator during the charge can be described as follows:

$$(OER\ mediator) \rightarrow (OER\ mediator)^+$$
$$+ e^- \quad (step\ 1,\ electrochemical\ reaction) \quad (9)$$

$$2(OER\ mediator)^+ + Li_2O_2 \rightarrow 2(OER\ mediator) + 2Li^+$$
$$+ O_2 \quad (step\ 2,\ chemical\ reaction) \quad (10)$$

Upon the charge, the OER mediator is electrochemically oxidized before the oxidation of $Li_2O_2$ following reaction (9). Successively, the oxidized OER mediator chemically decomposes $Li_2O_2$ into Li ions and oxygen (10), being reduced back to the initial state of the OER mediator. Because the OER mediator is not consumed in the reaction, even the addition of a small amount OER mediator in the electrolyte can, in principle, complete the charging reaction.

For the OER mediator to be active for $Li_2O_2$ decomposition, the redox potential of the OER mediator should be in a certain range. First, the redox potential of the (OER mediator)/(OER mediator)$^+$ should be higher than the theoretical formation potential of $Li_2O_2$ (2.96 V $vs.$ Li/Li$^+$) such that the (OER mediator)$^+$ is capable of chemically oxidizing $Li_2O_2$. Moreover, it is desirable that the redox potential of the (OER mediator)/(OER mediator)$^+$ be only slightly higher than 2.96 V ($vs.$ Li/Li$^+$) and lower than the typical oxidation potential of $Li_2O_2$ in the absence of a catalyst ($\sim$4.0 V $vs.$ Li/Li$^+$). These conditions would enable the OER mediator to be oxidized before $Li_2O_2$ with the lowest charging polarization. Since the first introduction of an OER mediator into Li–O$_2$ batteries,[62] several OER mediators have been recently proposed and have resulted in remarkable reductions of the charging overpotential. Fig. 7b lists some of the important OER mediators proposed to facilitate the decomposition of $Li_2O_2$ with their redox potentials plotted together with that of $Li_2O_2$ formation.[62,63,67,130–134] Although a detailed discussion of the performance of each OER mediator is beyond the scope of this review and can be found elsewhere,[44,62,131,134] it can be observed that the redox potential of the OER mediator itself has a clear correlation with the average charging voltages of Li–O$_2$ cells adopting each OER mediator. Moreover, the energy efficiency increases for the OER mediators with redox potentials closer to 2.96 V. This finding implies that the charging reaction of the Li–O$_2$ cells is governed by the electrochemical oxidation of the OER mediator and its chemical decomposition of $Li_2O_2$. Note that the redox potential of the OER mediator can vary depending on the environment, such as the solvent type and additives in the electrolyte.[53,135] This result is due to the possibly distinct solvation stability of the OER mediator and (OER mediator)$^+$. When the (OER mediator)$^+$ forms a more stable solvated complex with one particular electrolyte over another, the (OER mediator)/(OER mediator)$^+$ redox potential would differ in the two electrolytes. In addition, the selectivity of the OER mediator toward $Li_2O_2$ decomposition should be carefully considered. The OER mediator or (OER mediator)$^+$ can also react with cell components such as electrolytes other than $Li_2O_2$.[67,134] Lim et al. demonstrated that the relative electron

orbital energy states of the OER mediator or (OER mediator)$^+$ and the electrolyte molecule can guide the stability of the OER mediator in different types of electrolytes.[134] Apart from thermodynamic consideration of the reactivity of OER mediators, a kinetic aspect such as decomposition rate of $Li_2O_2$ of various OER mediators under different electrolytes should also be considered. For example, it was observed that the decomposition rate of oxidized OER mediator to $Li_2O_2$ alters depending on the combination of electrolyte and OER mediator.[136] A further study on the kinetics of OER mediators needs to be proceeded and it should be considered together with thermodynamic aspects to understand the overall activity of OER mediators under cell environments.

## Summary and outlook

In this progress article, we reviewed the recent findings and understanding concerning the reaction mechanisms occurring in Li–O$_2$ batteries and discussed the detailed reaction chemistries that are sensitively affected by various surrounding conditions. The role of the electrolyte is critical in determining not only the stability against oxygen radicals, as extensively studied in the early development of Li–O$_2$ batteries using carbonate-based electrolytes,[10,12] but also the discharge capacity and recharging capability $via$ regulation of either a solution-mediated process or surface-film formation during the discharge. An electrolyte with a strong solvation effect is beneficial with respect to the discharge capacity, as the stabilization of Li$^+$–O$_2^-$ in such an electrolyte could induce the solution-mediated reaction and trigger large discharge products. However, the stabilization effect results in an increased concentration of reactive O$_2^-$, promoting electrolyte decomposition. Addressing this trade-off between the capacity and electrolyte stability is important in selecting an appropriate electrolyte system. Moreover, solvents with high p$K_a$ values should be developed to resist side reactions with oxygen radicals and simultaneously induce a high discharge capacity. It should be also noted that mass transport properties, $i.e.$ the diffusion coefficient of O$_2$ and O$_2^-$, were also reported to affect the discharge mechanism, which should be carefully considered when designing the electrolyte system for Li–O$_2$ batteries.

In achieving both high energy density and energy efficiency, the capability of controlling the nature of the discharge product appears to be critical. Although the bulk growth of a discharge product with a toroidal morphology is beneficial for the discharge capacity, the charging process of such a product requires a high overpotential because of the insulating nature of $Li_2O_2$. To attain better energy efficiency without sacrificing the discharge capacity, the growth of large $Li_2O_2$ particles with enhanced electronic/ionic conductivities is needed. The introduction of defects such as Li vacancies in the crystalline $Li_2O_2$ or induction of an amorphous phase could be possible solutions.

Catalysts (solid/soluble) are also a key component with great potential to overcome the low-energy-efficiency issue. For solid catalysts, the operation mechanism is still elusive and controversial, while it affects the nature of the discharge products,

2884 | Chem. Soc. Rev., 2017, 46, 2873–2888

This journal is © The Royal Society of Chemistry 2017

thus influencing the charge/discharge of Li–O$_2$ cells. A fundamental understanding of this operation mechanism should thus be obtained before the development of new solid catalysts. Alternatively, soluble catalysts (*i.e.*, ORR/OER mediators) are considered to be a promising solution to simultaneously improve the energy efficiency and cell stability by altering the intermediate species and avoiding the generation of reactive O$_2^-$ or LiO$_2$. However, the selectivity of a soluble catalyst should be carefully considered to avoid side reactions with other cell components and shuttling issues. Also, the reaction kinetics of soluble catalysts for Li$_2$O$_2$ decomposition should be studied, which is related to the power capability of the cell. Further quantitative investigations on the kinetics and selectivity of soluble catalysts, *e.g.* turnover frequency or decomposition efficiency, are needed for a deeper understanding of catalytic activity.

The merits of Li–O$_2$ batteries originate from their seemingly simple chemistry, *i.e.*, $2Li^+ + O_2 + 2e^- \rightarrow Li_2O_2$. However, in practice, the reactions are not simple and involve multiple reaction pathways and side reactions; altering one component possibly results in a complete change in the reaction pathways. An in-depth understanding of the reaction and fine tuning of the cell components that regulate the desirable reaction pathway based on this understanding are the keys to expediting the development of high-energy-density Li–O$_2$ batteries with high rechargeability and efficiency.

## Acknowledgements

## Notes and references

1 P. G. Bruce, S. A. Freunberger, L. J. Hardwick and J.-M. Tarascon, *Nat. Mater.*, 2012, **11**, 19–29.
2 J. Lu, L. Li, J.-B. Park, Y.-K. Sun, F. Wu and K. Amine, *Chem. Rev.*, 2014, **114**, 5611–5640.
3 M. Balaish, A. Kraytsberg and Y. Ein-Eli, *Phys. Chem. Chem. Phys.*, 2014, **16**, 2801–2822.
4 D. Oh, J. Qi, Y.-C. Lu, Y. Zhang, Y. Shao-Horn and A. M. Belcher, *Nat. Commun.*, 2013, **4**, 2756.
5 J. Lu, Y. Jung Lee, X. Luo, K. Chun Lau, M. Asadi, H.-H. Wang, S. Brombosz, J. Wen, D. Zhai, Z. Chen, D. J. Miller, Y. Sub Jeong, J.-B. Park, Z. Zak Fang, B. Kumar, A. Salehi-Khojin, Y.-K. Sun, L. A. Curtiss and K. Amine, *Nature*, 2016, **529**, 377–382.
6 F. Cheng and J. Chen, *Chem. Soc. Rev.*, 2012, **41**, 2172–2192.
7 B. D. McCloskey, A. Speidel, R. Scheffler, D. C. Miller, V. Viswanathan, J. S. Hummelshøj, J. K. Nørskov and A. C. Luntz, *J. Phys. Chem. Lett.*, 2012, **3**, 997–1001.
8 Z. Peng, S. A. Freunberger, Y. Chen and P. G. Bruce, *Science*, 2012, **337**, 563–566.
9 M. M. Ottakam Thotiyl, S. A. Freunberger, Z. Peng and P. G. Bruce, *J. Am. Chem. Soc.*, 2012, **135**, 494–500.
10 S. A. Freunberger, Y. Chen, Z. Peng, J. M. Griffin, L. J. Hardwick, F. Bardé, P. Novák and P. G. Bruce, *J. Am. Chem. Soc.*, 2011, **133**, 8040–8047.
11 V. S. Bryantsev, V. Giordani, W. Walker, M. Blanco, S. Zecevic, K. Sasaki, J. Uddin, D. Addison and G. V. Chase, *J. Phys. Chem. A*, 2011, **115**, 12399–12409.
12 V. S. Bryantsev and M. Blanco, *J. Phys. Chem. Lett.*, 2011, **2**, 379–383.
13 L. Johnson, C. Li, Z. Liu, Y. Chen, S. A. Freunberger, P. C. Ashok, B. B. Praveen, K. Dholakia, J.-M. Tarascon and P. G. Bruce, *Nat. Chem.*, 2014, **6**, 1091–1099.
14 C. M. Burke, V. Pande, A. Khetan, V. Viswanathan and B. D. McCloskey, *Proc. Natl. Acad. Sci. U. S. A.*, 2015, **112**, 9293–9298.
15 F. Li, D.-M. Tang, Y. Chen, D. Golberg, H. Kitaura, T. Zhang, A. Yamada and H. Zhou, *Nano Lett.*, 2013, **13**, 4702–4707.
16 J. Lu, K. C. Lau, Y.-K. Sun, L. A. Curtiss and K. Amine, *J. Electrochem. Soc.*, 2015, **162**, A2439–A2446.
17 Z. Ma, X. Yuan, L. Li, Z.-F. Ma, D. P. Wilkinson, L. Zhang and J. Zhang, *Energy Environ. Sci.*, 2015, **8**, 2144–2198.
18 Z.-W. Chang, J.-J. Xu, Q.-C. Liu, L. Li and X.-B. Zhang, *Adv. Energy Mater.*, 2015, **5**, 1500633.
19 A. Khetan, A. Luntz and V. Viswanathan, *J. Phys. Chem. Lett.*, 2015, **6**, 1254–1259.
20 S. Wu, J. Tang, F. Li, X. Liu, Y. Yamauchi, M. Ishida and H. Zhou, *Adv. Funct. Mater.*, 2016, **26**, 3291–3298.
21 L. Lutz, W. Yin, A. Grimaud, D. Alves Dalla Corte, M. Tang, L. Johnson, E. Azaceta, V. Sarou-Kanian, A. J. Naylor, S. Hamad, J. A. Anta, E. Salager, R. Tena-Zaera, P. G. Bruce and J. M. Tarascon, *J. Phys. Chem. C*, 2016, **120**, 20068–20076.
22 F. S. Gittleson, R. E. Jones, D. K. Ward and M. E. Foster, *Energy Environ. Sci.*, 2017, DOI: 10.1039/C6EE02915A.
23 A. Khetan, H. Pitsch and V. Viswanathan, *J. Phys. Chem. Lett.*, 2014, **5**, 2419–2424.
24 V. S. Bryantsev, J. Uddin, V. Giordani, W. Walker, D. Addison and G. V. Chase, *J. Electrochem. Soc.*, 2013, **160**, A160–A171.
25 Y. Marcus, *Chem. Soc. Rev.*, 1993, **22**, 409–416.
26 H.-K. Lim, H.-D. Lim, K.-Y. Park, D.-H. Seo, H. Gwon, J. Hong, W. A. Goddard, H. Kim and K. Kang, *J. Am. Chem. Soc.*, 2013, **135**, 9733–9742.
27 D. Brouillette, G. Perron and J. E. Desnoyers, *J. Solution Chem.*, 1998, **27**, 151–182.
28 S. A. Freunberger, Y. Chen, N. E. Drewett, L. J. Hardwick, F. Bardé and P. G. Bruce, *Angew. Chem., Int. Ed.*, 2011, **50**, 8609–8613.
29 Y. Chen, S. A. Freunberger, Z. Peng, F. Bardé and P. G. Bruce, *J. Am. Chem. Soc.*, 2012, **134**, 7952–7957.
30 D. Xu, Z.-L. Wang, J.-J. Xu, L.-L. Zhang and X.-B. Zhang, *Chem. Commun.*, 2012, **48**, 6948–6950.
31 A. A. Frimer, T. Farkash-Solomon and G. Aljadeff, *J. Org. Chem.*, 1986, **51**, 2093–2098.
32 C. P. Andrieux, P. Hapiot and J. M. Saveant, *J. Am. Chem. Soc.*, 1987, **109**, 3768–3775.

This journal is © The Royal Society of Chemistry 2017

*Chem. Soc. Rev.*, 2017, **46**, 2873–2888 | **2885**

33 C. M. Collins, C. Sotiriou-Leventis, M. T. Canalas and N. Leventis, *Electrochim. Acta*, 2000, **45**, 2049–2059.

34 A. Khetan, H. Pitsch and V. Viswanathan, *J. Phys. Chem. Lett.*, 2014, **5**, 1318–1323.

35 W. Walker, V. Giordani, J. Uddin, V. S. Bryantsev, G. V. Chase and D. Addison, *J. Am. Chem. Soc.*, 2013, **135**, 2076–2079.

36 C. O. Laoire, S. Mukerjee, K. M. Abraham, E. J. Plichta and M. A. Hendrickson, *J. Phys. Chem. C*, 2009, **113**, 20127–20134.

37 C. O. Laoire, S. Mukerjee, K. M. Abraham, E. J. Plichta and M. A. Hendrickson, *J. Phys. Chem. C*, 2010, **114**, 9178–9186.

38 W. Fan, Z. Cui and X. Guo, *J. Phys. Chem. C*, 2013, **117**, 2623–2627.

39 B. D. McCloskey, R. Scheffler, A. Speidel, G. Girishkumar and A. C. Luntz, *J. Phys. Chem. C*, 2012, **116**, 23897–23905.

40 V. Viswanathan, J. K. Nørskov, A. Speidel, R. Scheffler, S. Gowda and A. C. Luntz, *J. Phys. Chem. Lett.*, 2013, **4**, 556–560.

41 M. J. Trahan, S. Mukerjee, E. J. Plichta, M. A. Hendrickson and K. M. Abraham, *J. Electrochem. Soc.*, 2013, **160**, A259–A267.

42 D. Sharon, D. Hirsberg, M. Salama, M. Afri, A. A. Frimer, M. Noked, W. Kwak, Y.-K. Sun and D. Aurbach, *ACS Appl. Mater. Interfaces*, 2016, **8**, 5300–5307.

43 N. B. Aetukuri, B. D. McCloskey, J. M. García, L. E. Krupp, V. Viswanathan and A. C. Luntz, *Nat. Chem.*, 2015, **7**, 50–56.

44 D. Aurbach, B. D. McCloskey, L. F. Nazar and P. G. Bruce, *Nat. Energy*, 2016, **1**, 16128.

45 E. Yilmaz, C. Yogi, K. Yamanaka, T. Ohta and H. R. Byon, *Nano Lett.*, 2013, **13**, 4679–4684.

46 P. Lou, C. Li, Z. Cui and X. Guo, *J. Mater. Chem. A*, 2016, **4**, 241–249.

47 S. Meini, M. Piana, N. Tsiouvaras, A. Garsuch and H. A. Gasteiger, *Electrochem. Solid-State Lett.*, 2012, **15**, A45–A48.

48 Z. Guo, X. Dong, S. Yuan, Y. Wang and Y. Xia, *J. Power Sources*, 2014, **264**, 1–7.

49 K. U. Schwenke, M. Metzger, T. Restle, M. Piana and H. A. Gasteiger, *J. Electrochem. Soc.*, 2015, **162**, A573–A584.

50 D. G. Kwabi, T. P. Batcho, S. Feng, L. Giordano, C. V. Thompson and Y. Shao-Horn, *Phys. Chem. Chem. Phys.*, 2016, **18**, 24944–24953.

51 S. Wu, J. Tang, F. Li, X. Liu and H. Zhou, *Chem. Commun.*, 2015, **51**, 16860–16863.

52 F. Li, S. Wu, D. Li, T. Zhang, P. He, A. Yamada and H. Zhou, *Nat. Commun.*, 2015, **6**, 7843.

53 T. Liu, M. Leskes, W. Yu, A. J. Moore, L. Zhou, P. M. Bayley, G. Kim and C. P. Grey, *Science*, 2015, **350**, 530–533.

54 W.-H. Ryu, F. S. Gittleson, M. Schwab, T. Goh and A. D. Taylor, *Nano Lett.*, 2014, **15**, 434–441.

55 B. G. Kim, H.-J. Kim, S. Back, K. W. Nam, Y. Jung, Y.-K. Han and J. W. Choi, *Sci. Rep.*, 2014, **4**, 4225.

56 C. Yang, R. A. Wong, M. Hong, K. Yamanaka, T. Ohta and H. R. Byon, *Nano Lett.*, 2016, **16**, 2969–2974.

57 R. Black, J. H. Lee, B. Adams, C. A. Mims and L. F. Nazar, *Angew. Chem.*, 2013, **125**, 410–414.

58 R. R. Mitchell, B. M. Gallant, Y. Shao-Horn and C. V. Thompson, *J. Phys. Chem. Lett.*, 2013, **4**, 1060–1064.

59 R. R. Mitchell, B. M. Gallant, C. V. Thompson and Y. Shao-Horn, *Energy Environ. Sci.*, 2011, **4**, 2952–2958.

60 H.-D. Lim, H. Song, H. Gwon, K.-Y. Park, J. Kim, Y. Bae, H. Kim, S.-K. Jung, T. Kim, Y. H. Kim, X. Lepro, R. Ovalle-Robles, R. H. Baughman and K. Kang, *Energy Environ. Sci.*, 2013, **6**, 3570–3575.

61 S. Sankarasubramanian, N. Singh, F. Mizuno and J. Prakash, *J. Power Sources*, 2016, **319**, 202–209.

62 Y. Chen, S. A. Freunberger, Z. Peng, O. Fontaine and P. G. Bruce, *Nat. Chem.*, 2013, **5**, 489–494.

63 H.-D. Lim, H. Song, J. Kim, H. Gwon, Y. Bae, K.-Y. Park, J. Hong, H. Kim, T. Kim, Y. H. Kim, X. Lepró, R. Ovalle-Robles, R. H. Baughman and K. Kang, *Angew. Chem., Int. Ed.*, 2014, **53**, 3926–3931.

64 S. Matsuda, K. Hashimoto and S. Nakanishi, *J. Phys. Chem. C*, 2014, **118**, 18397–18400.

65 M. J. Lacey, J. T. Frith and J. R. Owen, *Electrochem. Commun.*, 2013, **26**, 74–76.

66 X. Gao, Y. Chen, L. Johnson and P. G. Bruce, *Nat. Mater.*, 2016, **15**, 882–888.

67 D. Sun, Y. Shen, W. Zhang, L. Yu, Z. Yi, W. Yin, D. Wang, Y. Huang, J. Wang, D. Wang and J. B. Goodenough, *J. Am. Chem. Soc.*, 2014, **136**, 8941–8946.

68 S. Lau and L. A. Archer, *Nano Lett.*, 2015, **15**, 5995–6002.

69 B. M. Gallant, D. G. Kwabi, R. R. Mitchell, J. Zhou, C. V. Thompson and Y. Shao-Horn, *Energy Environ. Sci.*, 2013, **6**, 2518–2528.

70 B. D. Adams, C. Radtke, R. Black, M. L. Trudeau, K. Zaghib and L. F. Nazar, *Energy Environ. Sci.*, 2013, **6**, 1772–1778.

71 Y. Zhang, X. Zhang, J. Wang, W. C. McKee, Y. Xu and Z. Peng, *J. Phys. Chem. C*, 2016, **120**, 3690–3698.

72 Q.-C. Liu, J.-J. Xu, S. Yuan, Z.-W. Chang, D. Xu, Y.-B. Yin, L. Li, H.-X. Zhong, Y.-S. Jiang, J.-M. Yan and X.-B. Zhang, *Adv. Mater.*, 2015, **27**, 5241–5247.

73 J.-L. Shui, J. S. Okasinski, P. Kenesei, H. A. Dobbs, D. Zhao, J. D. Almer and D.-J. Liu, *Nat. Commun.*, 2013, **4**, 2255.

74 J.-J. Xu, Z.-L. Wang, D. Xu, L.-L. Zhang and X.-B. Zhang, *Nat. Commun.*, 2013, **4**, 2438.

75 R. S. Assary, J. Lu, P. Du, X. Luo, X. Zhang, Y. Ren, L. A. Curtiss and K. Amine, *ChemSusChem*, 2013, **6**, 51–55.

76 R. Mi, S. Li, X. Liu, L. Liu, Y. Li, J. Mei, Y. Chen, H. Liu, H. Wang, H. Yan and W.-M. Lau, *J. Mater. Chem. A*, 2014, **2**, 18746–18753.

77 L. Zhong, R. R. Mitchell, Y. Liu, B. M. Gallant, C. V. Thompson, J. Y. Huang, S. X. Mao and Y. Shao-Horn, *Nano Lett.*, 2013, **13**, 2209–2214.

78 A. Kushima, T. Koido, Y. Fujiwara, N. Kuriyama, N. Kusumi and J. Li, *Nano Lett.*, 2015, **15**, 8260–8265.

79 H. Zheng, D. Xiao, X. Li, Y. Liu, Y. Wu, J. Wang, K. Jiang, C. Chen, L. Gu and X. Wei, *Nano Lett.*, 2014, **14**, 4245–4249.

80 B. Lee, J. Kim, G. Yoon, H.-D. Lim, I.-S. Choi and K. Kang, *Chem. Mater.*, 2015, **27**, 8406–8413.

81  M. D. Radin and D. J. Siegel, *Energy Environ. Sci.*, 2013, **6**, 2370–2379.

82  J. Varley, V. Viswanathan, J. Nørskov and A. Luntz, *Energy Environ. Sci.*, 2014, **7**, 720–727.

83  O. Gerbig, R. Merkle and J. Maier, *Adv. Mater.*, 2013, **25**, 3129–3133.

84  J. Wang, Y. Zhang, L. Guo, E. Wang and Z. Peng, *Angew. Chem., Int. Ed.*, 2016, **55**, 5201–5205.

85  Y. Mo, S. P. Ong and G. Ceder, *Phys. Rev. B: Condens. Matter Mater. Phys.*, 2011, **84**, 205446.

86  J. Hummelshøj, A. Luntz and J. Nørskov, *J. Chem. Phys.*, 2013, **138**, 034703.

87  B. Lee, D.-H. Seo, H.-D. Lim, I. Park, K.-Y. Park, J. Kim and K. Kang, *Chem. Mater.*, 2014, **26**, 1048–1055.

88  G. Girishkumar, B. McCloskey, A. C. Luntz, S. Swanson and W. Wilcke, *J. Phys. Chem. Lett.*, 2010, **1**, 2193–2203.

89  H.-D. Lim, K.-Y. Park, H. Gwon, J. Hong, H. Kim and K. Kang, *Chem. Commun.*, 2012, **48**, 8374–8376.

90  A. Luntz, V. Viswanathan, J. Voss, J. Varley, J. Nørskov, R. Scheffler and A. Speidel, *J. Phys. Chem. Lett.*, 2013, **4**, 3494–3499.

91  Y.-C. Lu and Y. Shao-Horn, *J. Phys. Chem. Lett.*, 2012, **4**, 93–99.

92  Y. Wang, Z. Liang, Q. Zou, G. Cong and Y.-C. Lu, *J. Phys. Chem. C*, 2016, **120**, 6459–6466.

93  C. Xia, R. Black, R. Fernandes, B. Adams and L. F. Nazar, *Nat. Chem.*, 2015, **7**, 496–501.

94  P. Hartmann, M. Heinemann, C. L. Bender, K. Graf, R.-P. Baumann, P. Adelhelm, C. Heiliger and J. R. Janek, *J. Phys. Chem. C*, 2015, **119**, 22778–22786.

95  J. Kim, H. Park, B. Lee, W. M. Seong, H.-D. Lim, Y. Bae, H. Kim, W. K. Kim, K. H. Ryu and K. Kang, *Nat. Commun.*, 2016, **7**, 10670.

96  S. Ganapathy, B. D. Adams, G. Stenou, M. S. Anastasaki, K. Goubitz, X.-F. Miao, L. F. Nazar and M. Wagemaker, *J. Am. Chem. Soc.*, 2014, **136**, 16335–16344.

97  T. Ogasawara, A. Débart, M. Holzapfel, P. Novák and P. G. Bruce, *J. Am. Chem. Soc.*, 2006, **128**, 1390–1393.

98  Y.-C. Lu, D. G. Kwabi, K. P. Yao, J. R. Harding, J. Zhou, L. Zuin and Y. Shao-Horn, *Energy Environ. Sci.*, 2011, **4**, 2999–3007.

99  D. Zhai, H.-H. Wang, J. Yang, K. C. Lau, K. Li, K. Amine and L. A. Curtiss, *J. Am. Chem. Soc.*, 2013, **135**, 15364–15372.

100  J. Yang, D. Zhai, H.-H. Wang, K. C. Lau, J. A. Schlueter, P. Du, D. J. Myers, Y.-K. Sun, L. A. Curtiss and K. Amine, *Phys. Chem. Chem. Phys.*, 2013, **15**, 3764–3771.

101  H.-G. Jung, H.-S. Kim, J.-B. Park, I.-H. Oh, J. Hassoun, C. S. Yoon, B. Scrosati and Y.-K. Sun, *Nano Lett.*, 2012, **12**, 4333–4335.

102  J. Lu, Y. Lei, K. C. Lau, X. Luo, P. Du, J. Wen, R. S. Assary, U. Das, D. J. Miller, J. W. Elam, H. M. Albishri, D. A. El-Hady, Y.-K. Sun, L. A. Curtiss and K. Amine, *Nat. Commun.*, 2013, **4**, 2383.

103  F. Tian, M. D. Radin and D. J. Siegel, *Chem. Mater.*, 2014, **26**, 2952–2959.

104  M. D. Radin, C. W. Monroe and D. J. Siegel, *Chem. Mater.*, 2015, **27**, 839–847.

105  M. D. Radin, J. F. Rodriguez, F. Tian and D. J. Siegel, *J. Am. Chem. Soc.*, 2011, **134**, 1093–1103.

106  S. Kang, Y. Mo, S. P. Ong and G. Ceder, *Chem. Mater.*, 2013, **25**, 3328–3336.

107  L. Shi, A. Xu and T. Zhao, *Phys. Chem. Chem. Phys.*, 2015, **17**, 29859–29866.

108  G. Yang, Y. Wang and Y. Ma, *J. Phys. Chem. Lett.*, 2014, **5**, 2516–2521.

109  B. M. Gallant, D. G. Kwabi, R. R. Mitchell, J. Zhou, C. V. Thompson and Y. Shao-Horn, *Energy Environ. Sci.*, 2013, **6**, 2518–2528.

110  S. Ganapathy, J. R. Heringa, M. S. Anastasaki, B. D. Adams, M. van Hulzen, S. Basak, Z. Li, J. P. Wright, L. F. Nazar, N. H. van Dijk and M. Wagemaker, *J. Phys. Chem. Lett.*, 2016, **7**, 3388–3394.

111  Z. Li, S. Ganapathy, Y. Xu, J. R. Heringa, Q. Zhu, W. Chen and M. Wagemaker, *Chem. Mater.*, 2017, **29**, 1577–1586.

112  C. Xia, M. Waletzko, L. Chen, K. Peppler, P. J. Klar and J. R. Janek, *ACS Appl. Mater. Interfaces*, 2014, **6**, 12083–12092.

113  A. Dunst, V. Epp, I. Hanzu, S. Freunberger and M. Wilkening, *Energy Environ. Sci.*, 2014, **7**, 2739–2752.

114  Y. Zhang, Q. Cui, X. Zhang, W. C. McKee, Y. Xu, S. Ling, H. Li, G. Zhong, Y. Yang and Z. Peng, *Angew. Chem., Int. Ed.*, 2016, **55**, 10717–10721.

115  Y. Hu, X. Han, F. Cheng, Q. Zhao, Z. Hu and J. Chen, *Nanoscale*, 2013, **6**, 177–180.

116  A. Débart, A. J. Paterson, J. Bao and P. G. Bruce, *Angew. Chem.*, 2008, **120**, 4597–4600.

117  Y.-C. Lu, Z. Xu, H. A. Gasteiger, S. Chen, K. Hamad-Schifferli and Y. Shao-Horn, *J. Am. Chem. Soc.*, 2010, **132**, 12170–12171.

118  W.-H. Ryu, T.-H. Yoon, S. H. Song, S. Jeon, Y.-J. Park and I.-D. Kim, *Nano Lett.*, 2013, **13**, 4190–4197.

119  Z. Jian, P. Liu, F. Li, P. He, X. Guo, M. Chen and H. Zhou, *Angew. Chem., Int. Ed.*, 2014, **53**, 442–446.

120  Q.-C. Liu, J.-J. Xu, D. Xu and X.-B. Zhang, *Nat. Commun.*, 2015, **6**, 7892.

121  J.-J. Xu, D. Xu, Z.-L. Wang, H.-G. Wang, L.-L. Zhang and X.-B. Zhang, *Angew. Chem., Int. Ed.*, 2013, **52**, 3887–3890.

122  K. P. Yao, M. Risch, S. Y. Sayed, Y.-L. Lee, J. R. Harding, A. Grimaud, N. Pour, Z. Xu, J. Zhou and A. Mansour, *Energy Environ. Sci.*, 2015, **8**, 2417–2426.

123  K. U. Schwenke, S. Meini, X. Wu, H. A. Gasteiger and M. Piana, *Phys. Chem. Chem. Phys.*, 2013, **15**, 11830–11839.

124  S. Meini, S. Solchenbach, M. Piana and H. A. Gasteiger, *J. Electrochem. Soc.*, 2014, **161**, A1306–A1314.

125  Y. Yin, R. Zhao, Y. Deng and A. A. Franco, *J. Phys. Chem. Lett.*, 2017, **8**, 599–604.

126  S. Song, W. Xu, J. Zheng, L. Luo, M. H. Engelhard, M. E. Bowden, B. Liu, C.-M. Wang and J.-G. Zhang, *Nano Lett.*, 2017, **17**, 1417–1424.

127  S.-I. Okuoka, Y. Ogasawara, Y. Suga, M. Hibino, T. Kudo, H. Ono, K. Yonehara, Y. Sumida, Y. Yamada, A. Yamada, M. Oshima, E. Tochigi, N. Shibata, Y. Ikuhara and N. Mizuno, *Sci. Rep.*, 2014, **4**, 5684.

128 B. D. McCloskey, R. Scheffler, A. Speidel, D. S. Bethune, R. M. Shelby and A. C. Luntz, *J. Am. Chem. Soc.*, 2011, **133**, 18038–18041.

129 Y. S. Jeong, J.-B. Park, H.-G. Jung, J. Kim, X. Luo, J. Lu, L. Curtiss, K. Amine, Y.-K. Sun and B. Scrosati, *Nano Lett.*, 2015, **15**, 4261–4268.

130 W.-J. Kwak, D. Hirshberg, D. Sharon, H.-J. Shin, M. Afri, J.-B. Park, A. Garsuch, F. F. Chesneau, A. A. Frimer and D. Aurbach, *J. Mater. Chem. A*, 2015, **3**, 8855–8864.

131 B. J. Bergner, A. Schürmann, K. Peppler, A. Garsuch and J. Janek, *J. Am. Chem. Soc.*, 2014, **136**, 15054–15064.

132 N. Feng, P. He and H. Zhou, *ChemSusChem*, 2015, **8**, 600–602.

133 D. Kundu, R. Black, B. Adams and L. F. Nazar, *ACS Cent. Sci.*, 2015, **1**, 510–515.

134 H.-D. Lim, B. Lee, Y. Zheng, J. Hong, J. Kim, H. Gwon, Y. Ko, M. Lee, K. Cho and K. Kang, *Nat. Energy*, 2016, **1**, 16066.

135 B. Paduszek and M. K. Kalinowski, *Electrochim. Acta*, 1983, **28**, 639–642.

136 W. Zhang, Y. Shen, D. Sun, Z. Huang, J. Zhou, H. Yan and Y. Huang, *Nano Energy*, 2016, **30**, 43–51.

2888 | *Chem. Soc. Rev.*, 2017, **46**, 2873–2888

This journal is © The Royal Society of Chemistry 2017